JCI The Journal of Clinical Investigation

Survival signal REG3-α prevents crypt apoptosis to control acute gastrointestinal graft-versus-host disease

Dongchang Zhao, … , Pavan Reddy, James L.M. Ferrara

J Clin Invest. 2018. https://doi.org/10.1172/JCI99261.

Concise Communication In-Press Preview Immunology Transplantation

Graphical abstract

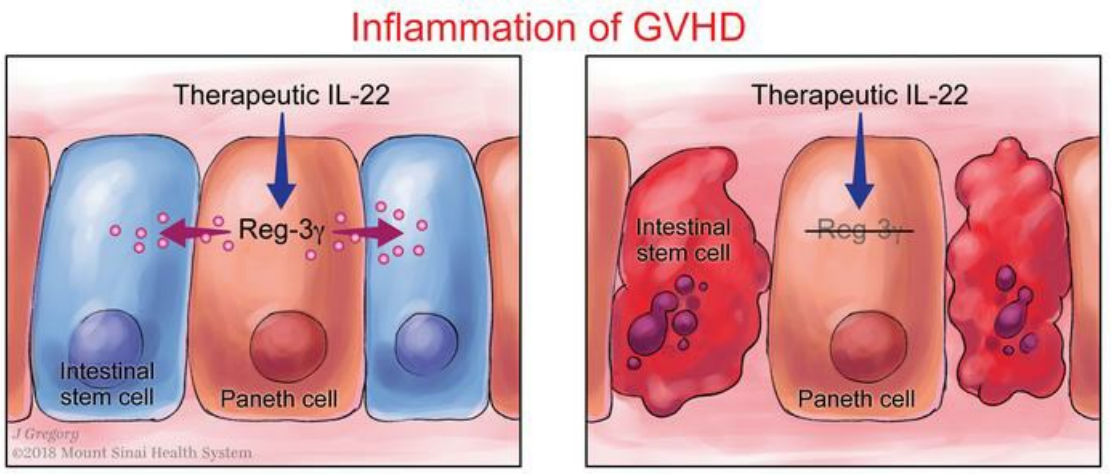

Title: Survival signal REG3α prevents crypt apoptosis to control acute gastrointestinal graft-versus-host disease

Authors: Dongchang Zhao[1]*, Yeung-Hyen Kim[2]*, Seihwan Jeong[1], Joel K. Greenson[3], Mohammed S. Chaudhry[1], Matthias Hoepting[4], Erik R. Anderson[1], Marcel R.M. van den Brink[5], Jonathan U. Peled[5], Antonio L.C. Gomes[5], Ann E. Slingerland[5], Michael J. Donovan[6], Andrew C. Harris[7], John E. Levine[1], Umut Ozbek[1], Lora V. Hooper[8], Thaddeus S. Stappenbeck[9], Aaron Ver Heul[9], Ta-Chiang Liu[9], Pavan Reddy[10], James L. M. Ferrara[1†]

Affiliations:

[1]The Tisch Cancer Institute and Division of Hematology / Medical Oncology, The Icahn School of Medicine at Mount Sinai Hospital, New York, NY, USA

[2]Department of Microbiology and Immunology, University of Michigan, Ann Arbor, MI, USA

[3]Department of Pathology, University of Michigan, Ann Arbor, MI, USA

[4]Department of Hematology, Hemostasis, Oncology and Stem Cell Transplantation, Hannover Medical School, Hannover, Germany

[5]Memorial Sloan Kettering Cancer Center, Weill Cornell Medical College, New York, NY, USA

[6]Department of Pathology, The Icahn School of Medicine at Mount Sinai Hospital, New York, NY, USA

[7]Blood and Marrow Transplantation Program, University of Utah, Salt Lake City, UT, USA

[8]Howard Hughes Medical Institute, Department of Immunology, University of Texas Southwestern Medical Center, Dallas, TX, USA

[9]Department of Pathology and Immunology, Washington University School of Medicine, MO, USA

[10]Division of Hematology/Oncology, University of Michigan, Ann Arbor, MI, USA

*DZ and YK contributed equally to this work.

†To whom correspondence should be addressed: James L. M. Ferrara, M.D., D.Sc., Hess Center for Science and Medicine, Icahn School of Medicine at Mount Sinai, Room S6-110, 1470 Madison Avenue, New York, NY 10029

Phone: 212-824-9365; Fax: 646-537-9567; Email: james.ferrara@mssm.edu

Competing Financial Interests: The authors declare no conflict of interest exists.

Abstract Graft-versus-host disease (GVHD) in the gastrointestinal (GI) tract remains the major cause of morbidity and non-relapse mortality after bone marrow transplantation (BMT). The Paneth cell protein, regenerating islet-derived 3-alpha (REG3α), is a biomarker specific for GI GVHD. REG3α serum levels rose in the systematic circulation as GVHD progressively destroyed Paneth cells and reduced GI epithelial barrier function. Paradoxically, GVHD suppressed intestinal REG3γ (the mouse homologue of human REG3α), and the absence of REG3γ in BMT recipients intensified GVHD but did not change the composition of the microbiome. IL-22 administration restored REG3γ production and prevented apoptosis of both intestinal stem cells (ISCs) and Paneth cells, but this protection was completely abrogated in *Reg3g*$^{-/-}$ mice. In vitro, addition of REG3α reduced the apoptosis of colonic cell lines. Strategies that increase intestinal REG3α/γ to promote crypt regeneration may offer a novel, non-immunosuppressive approach for GVHD and perhaps for other diseases involving the ISC niche such as inflammatory bowel disease.

Introduction

Acute graft-versus-host disease (GVHD) is the most serious complication of allogeneic bone marrow transplantation (BMT) and was noted in animal models more than six decades ago (1, 2). Acute GVHD predominantly involves the skin, liver, and lower gastrointestinal (GI) tract (3). Without rigorous depletion of donor T cells from the graft this complication occurs in 30%–70% of patients after allogeneic BMT (4-6). Standard treatment of acute GVHD is the administration of systemic corticosteroids and additional immunosuppressive agents; only half of patients who develop acute GVHD will have a complete response to corticosteroid therapy, although the numbers vary widely between studies (7). The outcome for patients with severe GVHD of the lower GI tract is poor, with 25% overall survival (8).We undertook this study to understand the biologic role of REG3α/γ in GI GVHD.

Results

An elevated REG3α blood level is a strong indicator of GI GVHD that drives transplant reported mortality (9-12). We observed that increased blood levels of REG3α in patients with GVHD inversely correlated with the number of Paneth cells **(Fig. 1A-C)** and observed a similar inverse correlation in two mouse models of GVHD **(Fig. 1D-I and Supplementary Fig. 1)**. This inverse correlation continued over time and increased with GVHD severity independently of BMT conditioning **(Fig. 2)**. IL-22 induces REG3γ (13-15) and the production of IL-22 decreased very rapidly during GVHD **(Fig. 2)**. Increased *Reg3g* expression was not observed in any other tissue, including lung, liver, and pancreas (data not shown) suggesting that damage to the GI crypt resulted in the loss of REG3γ into the systemic circulation. REG3α serum levels remained elevated, often by an order of magnitude after one week of systemic steroid therapy in patients

with GI GVHD and predicted increased non-relapse mortality, confirming the significance of continued serum elevations with respect to long term clinical outcomes **(Fig. 3)** (16).

We next investigated the role of REG3γ in GVHD using REG3γ deficient (*Reg3g*$^{-/-}$) mice as BMT recipients. *Reg3g*$^{-/-}$ mice experienced more severe clinical GVHD and greater mortality than wild type (WT) mice in two GVHD models **(Fig. 4A-C)**. The histologic severity of GVHD, as measured by Paneth cell apoptosis and loss, also increased in *Reg3g*$^{-/-}$ BMT recipients; so did the number of crypt cells expressing cleaved Caspase-3, a hallmark of apoptosis **(Fig. 4D-F and Supplementary Figs. 2,3)**. *Reg3g*$^{-/-}$ allogeneic BMT recipients also exhibited significantly more CD8^{+} IFNγ^{+} effector T cells in the lamina propria as well as increased hepatic infiltrates, confirming greater histologic damage in the absence of recipient REG3γ **(Supplementary Figs. 3,4)**. The composition of fecal microbial communities did not differ significantly, however, between WT and *Reg3g*$^{-/-}$BMT recipients either before transplant or during GVHD **(Fig. 4G-I and Supplementary Fig. 5)**.

Although IL-22 has pleiotropic effects and can increase GVHD severity in some models (17, 18), prophylactic administration of IL-22 prevented GVHD and increased REG3γ production in the ileum as previously reported (15) while simultaneously decreasing serum REG3γ levels **(Fig. 5 and Supplementary Fig. 6)**. IL-22 treatment of mice also reversed established GVHD in two separate models, and decreased release of REG3γ into serum **(Fig. 6, Supplementary Fig. 7)**. IL-22 was completely unable, however, to prevent clinical and histological GVHD and Paneth cell loss in *Reg3g*$^{-/-}$recipients in two separate models, confirming the need for REG3γ to repair the integrity of GI epithelium **(Fig. 7A,B and Supplementary Figs. 8-10)**. Other anti-microbial Paneth cell proteins that are disrupted during GVHD (19) such as *Defa1*, *Defa2*, *S100a8,* and

S100a9 mRNA expression did not consistently change in *Reg3g*$^{-/-}$recipients (**Supplementary Fig.11)**.

To investigate the effect of REG3γ on ISCs we bred *Reg3g*$^{-/-}$mice with mice heterozygous for green fluorescent protein (GFP) in LGR5^{+} enterocytes (20) to use as BMT recipients. We confirmed that the loss of ISCs during GVHD (21) was not reversed by IL-22 treatment in *Reg3g*$^{-/-}$mice (**Fig. 8A and Supplementary Fig. 12)**. We next quantified ISC apoptosis and proliferation using established flow cytometry protocols (22). Surprisingly, IL-22 did not affect ISC proliferation under any conditions, but reversed apoptosis only in WT and not in *Reg3g*$^{-/-}$recipients; the number of ISCs correlated directly with Reg3g mRNA expression (**Fig. 8B-D and Supplementary Figs. 13,14)**. We then directly evaluated the anti-apoptotic properties of REG3α on intestinal epithelium in vitro. Addition of REG3α in vitro to colonic epithelial cell lines undergoing apoptotic stress reduced the cleavage of caspases 3, 8, and PARP and increased cell viability in a dose-dependent manner, confirming its role as a survival factor for epithelial cells (**Fig. 8E-G and Supplementary Fig.15)**.

Discussion

We report here that the production of REG3α/γ in the GI tract falls as acute GVHD progresses and inversely correlates with its concentration in the serum, supporting the concept of this biomarker as a "liquid biopsy" that quantifies crypt damage and the loss of ISCs and Paneth cells. Administration of IL-22 restores GI epithelial integrity and reduces GVHD because REG3α/γ acts as a survival signal for ISCs and Paneth cells, preventing their apoptosis both in vitro and in vivo. The requirement of REG3α/γ to repair damaged GI epithelium treatment indicates a previously unknown function for this protein in GI crypt homeostasis.

These results suggest the possibility of a more physiologic approach to the prevention and treatment of GI GVHD through restoration of the GI mucosal barrier rather than intensified systemic immunosuppression. Paneth cells, the "guardians of the crypt", secrete multiple antimicrobial peptides, including REG proteins, that help to generate the chemical/physical barrier of the GI mucosa (23). A disrupted microbiome constitutes a significant risk factor for both experimental and clinical GVHD (24, 25) and might amplify GVHD by exposing enterocytes to Gram-positive pathogens (26). But analysis of the fecal microbiome demonstrated that the absence of REG3γ produced no significant difference in the microbial community architecture either before or during GVHD even though it caused greater crypt destruction and significantly increased the loss of ISCs and Paneth cells. This discrepancy suggested that the antimicrobial activity of REG3γ was not primarily responsible for its protective properties. Absence of host REG3γ thus amplified GVHD by accelerating apoptosis of the crypts, allowing microbes to break the mucosal epithelial barrier and activate antigen presenting cells that attracted and stimulated alloreactive donor T cells, furthering crypt damage (27).

Previous experiments with cultured pancreatic acinar cells and hepatocytes suggested that expression of REG3β could reduce the apoptosis mediated by TNFα, an important mediator of GVHD (28, 29). Our results directly demonstrate a survival function for REG3α/γ that is key to restoration of epithelial integrity during GVHD. A recently published approach to GVHD prevention is the promotion of Paneth cell development from ISCs through the administration of R-spondin-1, a Wnt agonist (30). It is unknown whether R-spondin-1 requires REG3γ to increase Paneth cell number as does IL-22. In this regard it is interesting to note that although IL-22 increases ISC number in vivo and stimulates organoid growth in vitro, it does not act as a mitogen as was initially thought; rather it prevents the apoptosis (or necroptosis) caused by the

inflammation of GVHD through the induction of REG3γ. Thus in addition to its well-defined antimicrobial properties, REG3γ provides critical survival signals to cells in the stem cell niche.

The potential limitations of this study should be noted. First, the mechanistic insights derive from mouse models and cell lines that cannot reproduce the complexity of human disease. Despite many tight correlations between human and murine data, some experiments do not and cannot have precise human equivalents, e.q. quantification of ISCs through a green fluorescent protein. Another important limitation relates to differences along the axial geography of the bowel. Both large and small intestines contain $Lgr5^+$ ISCs, but Paneth cells are largely absent in the colon where the stem cell niche is supported by deep secretory cells that possess some similarities to Paneth cells (31). Experiments are currently in progress to determine whether REG3γ also acts as a survival signal for colonic ISCs in vivo. If restoration of the survival signal provided by REG3γ can repair damage intestinal epithelium of both small and large intestines, this approach may offer a novel, non-immunosuppressive strategy not only for GVHD but for other immunologically mediated diseases of the bowel.

Materials and Methods

Patients. Patients were studied with the approval of the Institutional Review Boards at the University of Michigan and all patients gave written informed consent in accordance with the Declaration of Helsinki. Twenty-eight patients, who consented to a prospective observational trial of allogeneic BMT complications and underwent allogeneic BMT from 2002 to 2007, were available for analysis; samples were obtained from patients who developed GI symptoms, and had a duodenal biopsy and plasma collection at the time of onset of symptoms. All patients without GVHD had a histological grade of 0, and the median time of biopsy was day +37 (range

15-78); all those with GVHD had a histological grade of 3, and the median time of biopsy was day +65 (range 13-138).

Mice. C57BL/6 (B6; H-2^b, CD45.2^+), B6-Ly5.1 (H-2^b, CD45.1^+), B6 x DBA2 F1 (B6D2F1: H-$2^{b/d}$), and BALB/c (H-2^d, CD90.2) mice were purchased from Charles River Laboratories. C3H.SW (H-2^b, CD45.2^+) mice were purchased from the Jackson Laboratory. *Reg3g*$^{-/-}$(H-2^b) mice were obtained from Dr. Lora V. Hooper (26). B6-Lgr5-EGFP-IRES-creERT2 (Lgr5-EGFP$^+$) mice were a gift from Dr. Linda C. Samuelson of the University of Michigan at Ann Arbor. *Reg3g*$^{-/-}$mice were bred with wild type Lgr5-EGFP mice to generate dual *Reg3g*$^{-/-}$/Lgr5-EGFP mice (B6 background). For BMT experiments, WT and *Reg3g*$^{-/-}$recipient mice were cohoused for a minimum of two weeks, in order to reduce heterogeneity in the microbiota between the strains. All animals were cared for under the regulations reviewed and approved by the University Committee on the Use and Care of Animals, per University Laboratory Animal Medicine guidelines at the University of Michigan or the Icahn School of Medicine at Mount Sinai.

BMT. BMT was performed as previously described (32, 33). Briefly, bone marrow cells were collected from the femurs and tibias of euthanized donor mice. Donor T cells were obtained from the spleens of donor mice by positive selection using CD90.2 magnetic beads (Miltenyi Biotec), according to the manufacturer's instructions. Unless otherwise stated, B6D2F1 recipients were given a total of 1,250 cGy TBI, split into 2 doses separated by 4 hours on day -1, and then injected with 2-4 × 10^6 splenic T cells and 5 × 10^6 BM cells from allogeneic B6 donors on day 0. B6 recipients were irradiated with 1,100 cGy TBI, as a single dose on day -1, and injected on day 0 with 50 × 10^6 whole splenic cells and 5 × 10^6 BM cells from MHC-matched, minor antigen-

disparate C3H.SW donors or 5×10^6 whole splenic cells and 5×10^6 BM cells from MHC-mismatched BALB/c donors.

In all experiments, transplantation with cells from the appropriate syngeneic donor or bone marrow only was used as a control. Donor and recipient mice were sex-matched and were 8 to 16 weeks of age at the time of transplantation. Survival was monitored daily and clinical GVHD was assessed weekly by a previously described scoring system (34).

Administration of IL-22 *in vivo*. Recombinant mouse IL-22 (carrier-free) was purchased from BioLegend (San Diego, CA). For prophylaxis experiments, mice received IP injections of 10 μg of IL-22 in PBS, or PBS as a control, on alternate days from day +1 after BMT. Mice were given either 3 doses (when GI tissues were analyzed on day +7) or 6 doses (for longer term assessment of GVHD scores and survival).

To investigate the effect of treatment with IL-22 after development of GVHD, mice received IP injections of 10 μg of IL-22 in PBS, or PBS as a control, starting on day +7 after BMT. Mice were given either 3 daily doses (when GI tissues were analyzed on day +10) or a total of 7 total doses on days 7, 8, 9, 11, 13, 15, 17 (for longer term GVHD studies).

All animals were individually ear-tagged prior to BMT (4 animals per cage). At the time of randomization to receive IL-22 or PBS alone (day 0 for prophylaxis experiments and day 7 for treatment experiments), the first two mice were assigned to the IL-22 group and the second two mice were assigned to the PBS group. For experiments evaluating treatment beginning on day 7, animals with severe GVHD (weight loss of > 25%) were excluded prior to randomization. This criterion was established prior to BMT and the subsequent development of disease.

5-ethynyl-2'-deoxyuridine (EdU) incorporation *in vivo* assay. ISC proliferation was determined using EdU incorporation into DNA. Lgr5-EGFP$^+$ mice were injected

intraperitoneally with 200μL of 5mM EdU solution (Invitrogen) in PBS 2h before small intestinal samples were collected. EdU was detected with the Click-iT^{TM} Plus EdU Flow Cytometry Assay kit according to the manufacturer's instructions (Invitrogen).

Histopathology and immunohistochemistry. For pathologic analyses, samples from patients (duodenal biopsies) and mice (distal ilea and livers) were fixed in 10% neutral-buffered formalin, embedded in paraffin, sectioned, slide mounted, and stained with hematoxylin and eosin (12). Paneth cells were identified by their eosinophilic granules by an experienced observer blinded to the treatment groups, in at least 3 high-powered fields (HPFs) with an Olympus BX51 microscope. Using a highly reproducible technique (12), HPF was defined as a 40x objective with a field of 0.345 mm^2. The counts from each HPF were averaged to give the number of Paneth cells per HPF.

Immunohistochemistry was performed with polyclonal rabbit anti-REG3α (Abcam, ab134309) at a 1:200 dilution for human samples and rabbit anti-REG3γ from Dr. Lora V. Hooper lab (26)) at a 1:8000 dilution or rabbit anti-cleaved caspase-3 (Clone 5A1E, Cell Signaling) at a 1:400 dilution for murine sample using a DAKO AutoStainer Link (Dako, Carpinteria, CA); slides were subsequently coated with a goat anti-rabbit IgG HRP conjugate (DAKO) at a 1:200 dilution and finally a diaminobenzide (DAB) dilution to generate brown colored signals. Slides were counterstained with Harris Hematoxylin. Semiquantitative REG3α expression from duodenum biopsies was scored on a 0-2 scale for three parameters: Paneth cells, epithelial cytoplasm and stromal cells. Pictures from tissue sections were taken using a digital camera (DP70; Olympus) mounted on a microscope (BX51; Olympus) or EVOS XL Core Imaging System from Life Technologies.

Quantitative PCR (qPCR). Total RNA was isolated from the small intestine using the RNeasy RNA Isolation Kit (Qiagen) and was used to synthesize cDNA with the High-Capacity cDNA Reverse Transcription Kit (Applied Biosystems). qPCR analysis was performed using the SYBR Green Master Mix (Invitrogen) and specific primers. Signals were normalized to *Gapdh* levels within each sample and normalized data were used to calculate relative levels of gene expression using $\Delta\Delta C_t$ analysis. Details of all primers used can be found in Supplementary Table 1.

Enzyme-linked immunosorbent assay (ELISA). REG3α in human plasma was quantified with the REG3α ELISA kit (MBL International, Japan) as described previously (11). REG3γ in mice serum was measured by a REG3γ ELISA Kit (Cloud-Clone Corp, Houston, TX) and performed according to the manufacturer's protocol. Absorbance was measured with a SpectraMax M2 (Molecular Devices), and results were calculated with SoftMax Pro Version 5.4 software (Molecular Devices).

Western blot. HT-29 cells were treated with human recombinant Reg3α protein (R&D Systems, 5940-RG-050) (1000ng/ml) followed by Birinapant (10nM) and rhTNFα (10ng/ml) treatment for various time points (4, 8 and 16 hours). Cells were lysed in RIPA buffer containing protease and phosphatase inhibitors and sonicated with Bioruptor (Diagenode). Analysis was performed on total cell lysate. Protein was quantified using Pierce rapid gold BCA protein assay kit (ThermoFisher). 30μg of lysate was loaded onto NuPAGE 4-12% Bis-Tris protein gel or 12% Bis-Tris protein gel and protein was separated by electrophoresis followed by transferring into nitrocellulose membrane. Membranes were blocked for 1 hour at room temperature with TBST and 5% non-fat milk and incubated overnight at 4°C with the following primary antibodies (Cell Signaling): PARP (9532S), cleaved PARP (5625S), Caspase-8 (9746S), Caspase-3 (29629S), cleaved Caspase-3 (9661S) and β-actin (5125S). Proteins were detected with Pierce ECL

Western Blotting Substrate (ThermoFisher) or Lumigen ECL Ultra (Lumigen) following 1 hour incubation at room temperature with antibodies (Cell Signaling) anti-rabbit HRP (7074S) or anti-mouse HRP (7076S).

Apoptosis induced colorectal epithelial cell viability measurement. 2.5 x 10^5 cells of the colorectal cell line HT-29 were cultured in serum deprived DMEM medium overnight. Human recombinant REG3α protein (R&D Systems, 5940-RG-050) (10, 100 and 1000ng/ml) was added to culture for 2 hours and apoptosis was induced by then adding Birinapant (10nM) and rhTNFα (10ng/ml) to the culture for 24 hours. Cell viability was measured by CellTiter-Glo 2.0 assay kit (Promega) according to the manufacturer's protocol. Luminescence was measured with a SpectraMax M2 (Molecular Devices).

LPL isolation. LPLs from **s**mall intestines were isolated as described previously (26). Briefly, 5 cm distal ileum was opened longitudinally, and rinsed in cold PBS, cut into 5 mm pieces and washed twice with 2 mM EDTA (Fisher Scientific) and 1 mM DTT (Fisher Scientific) in serum free RPMI (Sigma) for 15 minutes at 37ºC in a shaker at 150 rpm. Tissues were then washed with PBS supplemented with 3% FBS (Sigma) in a 100 µm cell strainer. Tissue was then cut into 1-3mm pieces and incubated in a solution containing RPMI, 2% FBS, 3.7u Liberase TM (Roche), and 400u DNAse1 (Sigma) for 15 minutes in an orbital shaker under the same conditions as above. Tissues were subsequently serial filtered through a 70 µm and a 40 µm cell strainer using ice cold PBS, and LPLs were isolated after centrifugation on a Percoll gradient (GE Healthcare).

Intestinal crypt isolation and single cell dissociation. Isolation of mouse intestinal crypts and dissociation of cells for analysis by flow cytometry was performed as previously described (35). Briefly, 5 cm proximal duodenum was opened longitudinally, rinsed in cold PBS and cut into 5

mm pieces. To detach the crypts, small intestine pieces were incubated on ice in 10 mM EDTA (Fisher Scientific) for 30 minutes. Intestine was then resuspended vigorously in PBS, leading to supernatant enriched in crypts, which was subsequently filtered through a 70 μm cell strainer. Following centrifugation of isolated crypts, the pellet was disaggregated into single cells by incubation for 5 minutes with pre-warmed (37ºC) 1× TrypLE express (Gibco, Life Technologies), supplemented with 10 μM ROCK Inhibitor Y27632 dihydrochloride (Fisher Scientific) and 0.5 mM N-acetylcysteine (Sigma).

Flow cytometry. After isolation, LPLs were further incubated with Cell Stimulation Cocktail (eBioscience) for 4 hours, and 1 x 10^6 cells were subsequently surface-stained with CD4, CD8, and TCRβ antibodies. For detection of polarized T cell subsets, cells were incubated overnight at 4ºC in 400 μL of Fix/Perm solution (BD Biosciences), and then stained in Perm/Wash buffer (BD Biosciences) with IFNγ, IL-10 and IL-17A antibodies. For detection of Tregs, surface-stained LPLs were stained with FoxP3 antibody using the Foxp3 / Transcription Factor Staining Buffer Set (eBioscience). Isolated, dissociated intestinal crypt cells were surface-stained with EpCAM, CD45, CD31, TER-119 and CD24 antibodies. Apoptotic intestinal crypt cells were detected by using the Annexin V Apoptosis Detection Kit (eBioscience). DAPI, 7-AAD and Fixable Live/Dead Cell Stain Kits (Invitrogen) were used for viability staining. All flow cytometry was performed on a FACSCanto or LSR Fortessa, using FACSDiva software (all BD Biosciences). Data were analyzed using FlowJo software (TreeStar). Full details of all antibodies used are in Supplementary Table 1.

16S Sequencing. DNA from fecal pellets of individual mice were frozen until DNA was extracted by mechanical disruption (bead-beating) in phenol-chloroform. The V4-V5 region of

the ribosomal RNA gene was amplified, sequenced, and computationally analyzed as described (36, 37).

Statistical analysis. Statistical analysis was performed and graphs were generated using Prism software (GraphPad). Survival curves were plotted using Kaplan-Meier estimates and compared by using the log-rank test. For survival experiments, a sample size of 7 per group provided 80% power to detect survival benefit of at least 40% with an alpha of 0.05. For comparison of two groups, an unpaired two-tailed t-test for parametric data was used. In the case of multiple comparisons, one-way analysis of variance (ANOVA) with Bonferroni correction was used. Principal Component Analysis was performed using the R package, and Bray-Curtis compositional distances were compared using a Wilcox test. All data were tested for normality through application of the F test with Prism software, and all tests were two-sided. Differences were considered significant when the P value was <0.05. Data are always presented as mean and SEM for the different groups. Unless otherwise specified, all studies for which data are presented are representative of at least two independent experiments.

Study Approval Human blood samples study was approved by Icahn School of Medicine at Mount Sinai (IRB# 15-0093). Mouse research project was approved by Icahn School of Medicine at Mount Sinai (IACUC# 2014-0202).

Author Contributions

D.Z., Y.K. and J.L.M.F. designed the study. D.Z., Y.K., S.J., J.K.G., M.S.C., M.H., E.R.A., M.v.d.B., J.U.P., A.L.C.G., A.E.S., M.J.D., A.C.H., J.E.L., U.O., T.S.S., A.V.H., T.L. and P.R.

performed the experiments and analysis. L.V.H. provided key reagents. D.Z., M.S.C. and J.L.M.F. prepared the manuscript with input from all authors.

Acknowledgments

The authors thank the physicians and data management teams of the BMT Program at the University of Michigan and the University of Regensburg. **Funding**: This work was supported by National Institutes of Health grants P01-CA039542 (J.L.M.F.), 5T32AI078892 (E.R.A.), R01-CA228358 and R01-CA228308 (M.v.d.B.), American Cancer Society CRP-13-306-06-COUN (J.L.M.F.), and Deutscher Akademischer Austauschdienst (M.H.).

References

1. Billingham RE. The biology of graft-versus-host reactions. *Harvey lectures.* 1966;62:21-78.
2. Gatti RA, Kersey JH, Yunis EJ, and Good RA. Graft-versus-host disease. *Progress in clinical pathology.* 1973;5:1-18.
3. Weisdorf DJ, Snover DC, Haake R, Miller WJ, McGlave PB, Blazar B, Ramsay NK, Kersey JH, and Filipovich A. Acute upper gastrointestinal graft-versus-host disease: clinical significance and response to immunosuppressive therapy. *Blood.* 1990;76(3):624-9.
4. Przepiorka D, Smith TL, Folloder J, Khouri I, Ueno NT, Mehra R, Korbling M, Huh YO, Giralt S, Gajewski J, et al. Risk factors for acute graft-versus-host disease after allogeneic blood stem cell transplantation. *Blood.* 1999;94(4):1465-70.

5. Verneris MR, Lee SJ, Ahn KW, Wang HL, Battiwalla M, Inamoto Y, Fernandez-Vina MA, Gajewski J, Pidala J, Munker R, et al. HLA Mismatch Is Associated with Worse Outcomes after Unrelated Donor Reduced-Intensity Conditioning Hematopoietic Cell Transplantation: An Analysis from the Center for International Blood and Marrow Transplant Research. *Biology of blood and marrow transplantation : journal of the American Society for Blood and Marrow Transplantation.* 2015;21(10):1783-9.

6. Pidala J, Wang T, Haagenson M, Spellman SR, Askar M, Battiwalla M, Baxter-Lowe LA, Bitan M, Fernandez-Vina M, Gandhi M, et al. Amino acid substitution at peptide-binding pockets of HLA class I molecules increases risk of severe acute GVHD and mortality. *Blood.* 2013;122(22):3651-8.

7. Westin JR, Saliba RM, De Lima M, Alousi A, Hosing C, Qazilbash MH, Khouri IF, Shpall EJ, Anderlini P, Rondon G, et al. Steroid-Refractory Acute GVHD: Predictors and Outcomes. *Advances in Hematology.* 2011;2011: 601953.

8. Castilla-Llorente C, Martin PJ, McDonald GB, Storer BE, Appelbaum FR, Deeg HJ, Mielcarek M, Shulman H, Storb R, and Nash RA. Prognostic factors and outcomes of severe gastrointestinal GVHD after allogeneic hematopoietic cell transplantation. *Bone Marrow Transplantation.* 2014;49(7):966-71.

9. Hill GR, and Ferrara JL. The primacy of the gastrointestinal tract as a target organ of acute graft-versus-host disease: rationale for the use of cytokine shields in allogeneic bone marrow transplantation. *Blood.* 2000;95(9):2754-9.

10. MacMillan ML, DeFor TE, and Weisdorf DJ. What predicts high risk acute graft-versus-host disease (GVHD) at onset?: identification of those at highest risk by a novel acute GVHD risk score. *British Journal of Haematology.* 2012;157(6):732-41.

11. Ferrara JL, Harris AC, Greenson JK, Braun TM, Holler E, Teshima T, Levine JE, Choi SW, Huber E, Landfried K, et al. Regenerating islet-derived 3-alpha is a biomarker of gastrointestinal graft-versus-host disease. *Blood.* 2011;118(25):6702-8.

12. Levine JE, Huber E, Hammer ST, Harris AC, Greenson JK, Braun TM, Ferrara JL, and Holler E. Low Paneth cell numbers at onset of gastrointestinal graft-versus-host disease identify patients at high risk for nonrelapse mortality. *Blood.* 2013;122(8):1505-9.

13. Zheng Y, Valdez PA, Danilenko DM, Hu Y, Sa SM, Gong Q, Abbas AR, Modrusan Z, Ghilardi N, de Sauvage FJ, et al. Interleukin-22 mediates early host defense against attaching and effacing bacterial pathogens. *Nature Medicine.* 2008;14(3):282-9.

14. Sanos SL, Bui VL, Mortha A, Oberle K, Heners C, Johner C, and Diefenbach A. RORgammat and commensal microflora are required for the differentiation of mucosal interleukin 22-producing NKp46+ cells. *Nature Immunology.* 2009;10(1):83-91.

15. Hanash AM, Dudakov JA, Hua G, O'Connor MH, Young LF, Singer NV, West ML, Jenq RR, Holland AM, Kappel LW, et al. Interleukin-22 protects intestinal stem cells from immune-mediated tissue damage and regulates sensitivity to graft versus host disease. *Immunity.* 2012;37(2):339-50.

16. Major-Monfried H, Renteria AS, Pawarode A, Reddy P, Ayuk F, Holler E, Efebera YA, Hogan WJ, Wolfl M, Qayed M, et al. MAGIC biomarkers predict long-term outcomes for steroid-resistant acute GVHD. *Blood.* 2018;131(25):2846-55.

17. Couturier M, Lamarthee B, Arbez J, Renauld JC, Bossard C, Malard F, Bonnefoy F, Mohty M, Perruche S, Tiberghien P, et al. IL-22 deficiency in donor T cells attenuates murine acute graft-versus-host disease mortality while sparing the graft-versus-leukemia effect. *Leukemia.* 2013;27(7):1527-37.

18. Zhao K, Zhao D, Huang D, Yin L, Chen C, Pan B, Wu Q, Li Z, Yao Y, Shen E, et al. Interleukin-22 aggravates murine acute graft-versus-host disease by expanding effector T cell and reducing regulatory T cell. *Journal of Interferon & Cytokine Research : The Official Journal of the International Society for Interferon and Cytokine Research.* 2014;34(9):707-15.

19. Eriguchi Y, Takashima S, Oka H, Shimoji S, Nakamura K, Uryu H, Shimoda S, Iwasaki H, Shimono N, Ayabe T, et al. Graft-versus-host disease disrupts intestinal microbial ecology by inhibiting Paneth cell production of alpha-defensins. *Blood.* 2012;120(1):223-31.

20. Barker N, van Es JH, Kuipers J, Kujala P, van den Born M, Cozijnsen M, Haegebarth A, Korving J, Begthel H, Peters PJ, et al. Identification of stem cells in small intestine and colon by marker gene Lgr5. *Nature.* 2007;449(7165):1003-7.

21. Lindemans CA, Calafiore M, Mertelsmann AM, O'Connor MH, Dudakov JA, Jenq RR, Velardi E, Young LF, Smith OM, Lawrence G, et al. Interleukin-22 promotes intestinal-stem-cell-mediated epithelial regeneration. *Nature.* 2015;528(7583):560-4.

22. Vermes I, Haanen C, Steffens-Nakken H, and Reutelingsperger C. A novel assay for apoptosis. Flow cytometric detection of phosphatidylserine expression on early apoptotic cells using fluorescein labelled Annexin V. *Journal of Immunological Methods.* 1995;184(1):39-51.

23. Ganz T. Paneth cells--guardians of the gut cell hatchery. *Nature Immunology.* 2000;1(2):99-100.

24. Jenq RR, Ubeda C, Taur Y, Menezes CC, Khanin R, Dudakov JA, Liu C, West ML, Singer NV, Equinda MJ, et al. Regulation of intestinal inflammation by microbiota

following allogeneic bone marrow transplantation. *The Journal of Experimental Medicine.* 2012;209(5):903-11.

25. Weber D, Oefner PJ, Hiergeist A, Koestler J, Gessner A, Weber M, Hahn J, Wolff D, Stammler F, Spang R, et al. Low urinary indoxyl sulfate levels early after transplantation reflect a disrupted microbiome and are associated with poor outcome. *Blood.* 2015;126(14):1723-8.

26. Vaishnava S, Yamamoto M, Severson KM, Ruhn KA, Yu X, Koren O, Ley R, Wakeland EK, and Hooper LV. The antibacterial lectin RegIIIgamma promotes the spatial segregation of microbiota and host in the intestine. *Science.* 2011;334(6053):255-8.

27. Zeiser R, and Blazar BR. Acute Graft-versus-Host Disease - Biologic Process, Prevention, and Therapy. *The New England journal of medicine.* 2017;377(22):2167-79.

28. Malka D, Vasseur S, Bodeker H, Ortiz EM, Dusetti NJ, Verrando P, Dagorn JC, and Iovanna JL. Tumor necrosis factor alpha triggers antiapoptotic mechanisms in rat pancreatic cells through pancreatitis-associated protein I activation. *Gastroenterology.* 2000;119(3):816-28.

29. Simon MT, Pauloin A, Normand G, Lieu HT, Mouly H, Pivert G, Carnot F, Tralhao JG, Brechot C, and Christa L. HIP/PAP stimulates liver regeneration after partial hepatectomy and combines mitogenic and anti-apoptotic functions through the PKA signaling pathway. *FASEB Journal : Official Publication of the Federation of American Societies for Experimental Biology.* 2003;17(11):1441-50.

30. Hayase E, Hashimoto D, Nakamura K, Noizat C, Ogasawara R, Takahashi S, Ohigashi H, Yokoi Y, Sugimoto R, Matsuoka S, et al. R-Spondin1 expands Paneth cells and prevents

dysbiosis induced by graft-versus-host disease. *The Journal of Experimental Medicine.* 2017;214(12):3507-18.

31. Sasaki N, Sachs N, Wiebrands K, Ellenbroek SI, Fumagalli A, Lyubimova A, Begthel H, van den Born M, van Es JH, Karthaus WR, et al. Reg4+ deep crypt secretory cells function as epithelial niche for Lgr5+ stem cells in colon. *Proceedings of the National Academy of Sciences of the United States of America.* 2016;113(37):E5399-407.

32. Teshima T, Ordemann R, Reddy P, Gagin S, Liu C, Cooke KR, and Ferrara JL. Acute graft-versus-host disease does not require alloantigen expression on host epithelium. *Nature Medicine.* 2002;8(6):575-81.

33. Reddy P, Maeda Y, Liu C, Krijanovski OI, Korngold R, and Ferrara JL. A crucial role for antigen-presenting cells and alloantigen expression in graft-versus-leukemia responses. *Nature Medicine.* 2005;11(11):1244-9.

34. Cooke KR, Gerbitz A, Crawford JM, Teshima T, Hill GR, Tesolin A, Rossignol DP, and Ferrara JL. LPS antagonism reduces graft-versus-host disease and preserves graft-versus-leukemia activity after experimental bone marrow transplantation. *The Journal of Clinical Investigation.* 2001;107(12):1581-9.

35. Sato T, van Es JH, Snippert HJ, Stange DE, Vries RG, van den Born M, Barker N, Shroyer NF, van de Wetering M, and Clevers H. Paneth cells constitute the niche for Lgr5 stem cells in intestinal crypts. *Nature.* 2011;469(7330):415.

36. Staffas A, Burgos da Silva M, Slingerland AE, Lazrak A, Bare CJ, Holman CD, Docampo MD, Shono Y, Durham B, Pickard AJ, et al. Nutritional Support from the Intestinal Microbiota Improves Hematopoietic Reconstitution after Bone Marrow Transplantation in Mice. *Cell Host & Microbe.* 2018;23(4):447-57.e4.

37. Shono Y, Docampo MD, Peled JU, Perobelli SM, Velardi E, Tsai JJ, Slingerland AE, Smith OM, Young LF, Gupta J, et al. Increased GVHD-related mortality with broad-spectrum antibiotic use after allogeneic hematopoietic stem cell transplantation in human patients and mice. *Science Translational Medicine.* 2016;8(339):339ra71.

Figures and Figure Legends

Figure 1

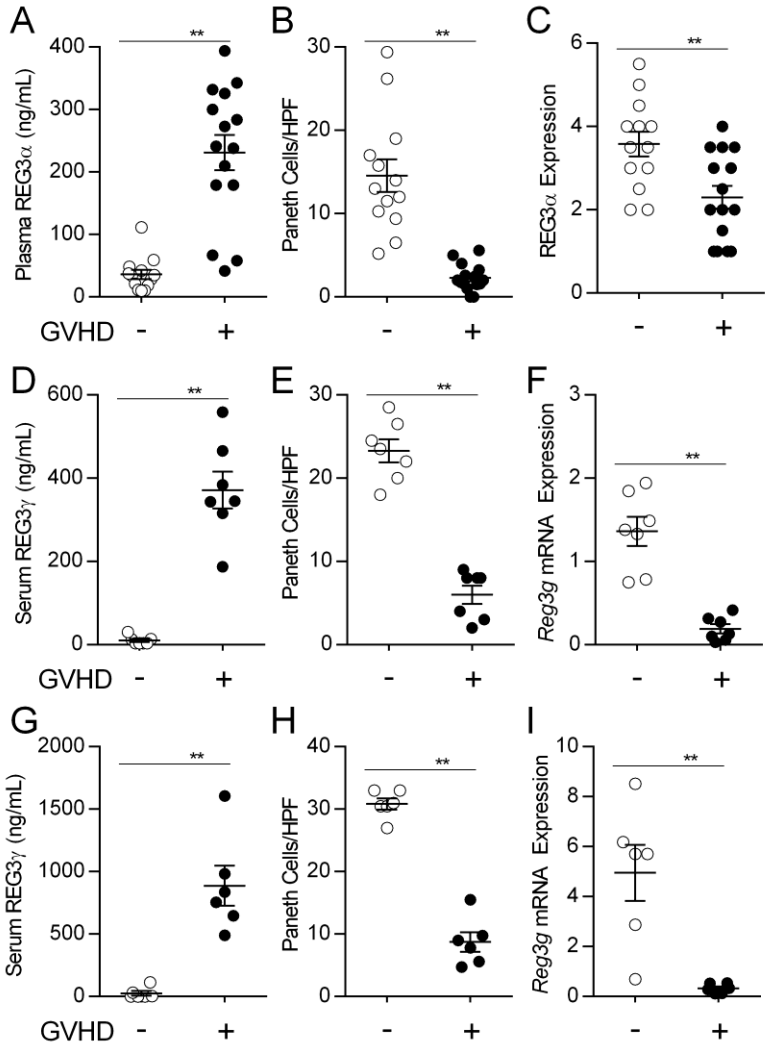

Figure 1. REG3α/γ levels in the plasma/serum and intestinal mucosa during GVHD. (A-C) Samples were collected from 28 allogeneic BMT patients without GVHD (○, n=13) and with GVHD (●, n=15). **(A)** Plasma concentrations of REG3α measured by ELISA. **(B)** Average Paneth cell numbers per high power field (HPF) in the same biopsies. **(C)** Semiquantitative REG3α expression in the duodenum. **(D-F)** B6 mice underwent BMT from syngeneic B6-Ly5.1 donors (GVHD − ○, n=7) or allogeneic C3H.SW donors (GVHD + ●, n=7), and samples were analyzed on day +7 after BMT. **(D)** Serum REG3γ levels measured by ELISA. **(E)** Average Paneth cell numbers per high power field (HPF) in ileal tissue from the same mice. **(F)** Ileal tissue *Reg3g* mRNA expression measured by qPCR. **(G-I)** B6D2F1 mice underwent BMT from syngeneic B6D2F1 donors (GVHD − ○, n=6) or allogeneic B6 donors (GVHD + ●, n=6), and samples were analyzed as before on day +7 after BMT. **(G)** Serum REG3γ levels, **(H)** Average Paneth cell numbers per high power field (HPF) in ileal tissue, and **(I)** Ileal tissue *Reg3g* mRNA expression**.** **P<0.01, unpaired two-tailed *t* test. Data are expressed as mean ±SEM.

Figure 2

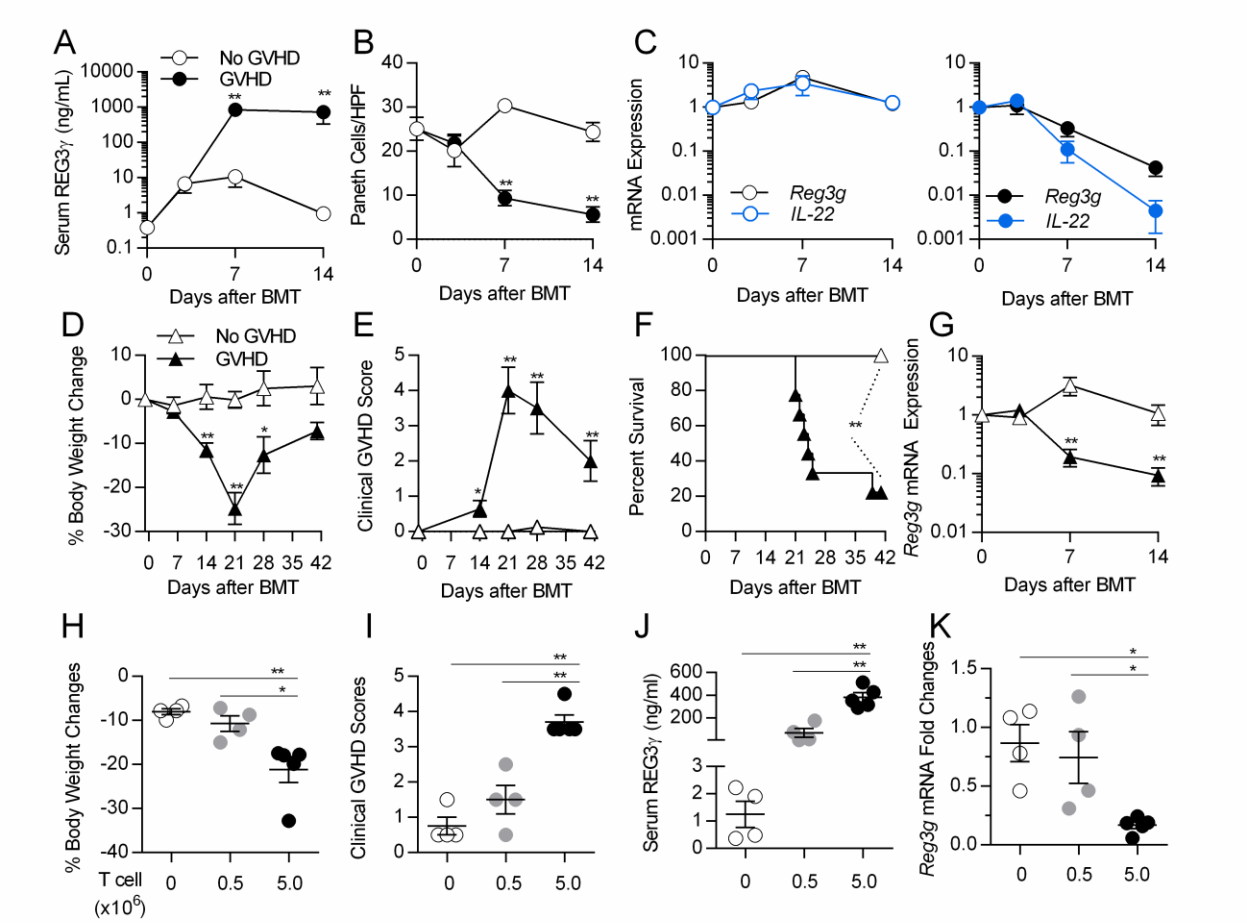

Figure 2. Time course of REG3γ and IL-22 expression during GVHD. **(A-C)** B6D2F1 mice underwent BMT from syngeneic B6D2F1 donors (No GVHD, ○) or allogeneic B6 donors (GVHD, ●), and samples were analyzed on days +3, +7 and +14 after BMT (n=5 for each group on each day). (**A**) Serial REG3γ levels in the serum as measured by ELISA, (**B**) Serial average Paneth cell numbers per high power field (HPF) in ileal tissue, and (**C**) Serial *Reg3g* and *IL-22* mRNA expression in the ileum was measured by qPCR. (**D-G**) B6D2F1 mice underwent BMT, without irradiation conditioning, from syngeneic B6D2F1 donors (No GVHD, ○) or allogeneic B6 donors (GVHD, ●). (**D**) Serial body weight measurement, (**E**) Clinical GVHD score and (**F**) Survival of mice after BMT. **P<0.01, log-rank test. (**G**) Serial *Reg3g* mRNA expression in the ileum on days +3, +7 and +14 after BMT (n=6 for each group on each day. *P<0.05, **P<0.01, unpaired two-tailed *t* test (**A-E,G**). **(H-K)** Following irradiation, B6 mice received C3H.SW donors with 5.0x10^6 of bone marrow cells plus 0-5.0x10^6 of T cells as indicated. Samples were analyzed on day +7 after BMT (n=4 for each group). **(H)** Body weight measurement, **(I)** Clinical GVHD score, **(J)** Serum REG3γ levels and **(K)** *Reg3g* mRNA expression in the ileum. *P<0.05, **P<0.01, one-way analysis of variance (ANOVA). Data are expressed as mean ±SEM.

Figure 3

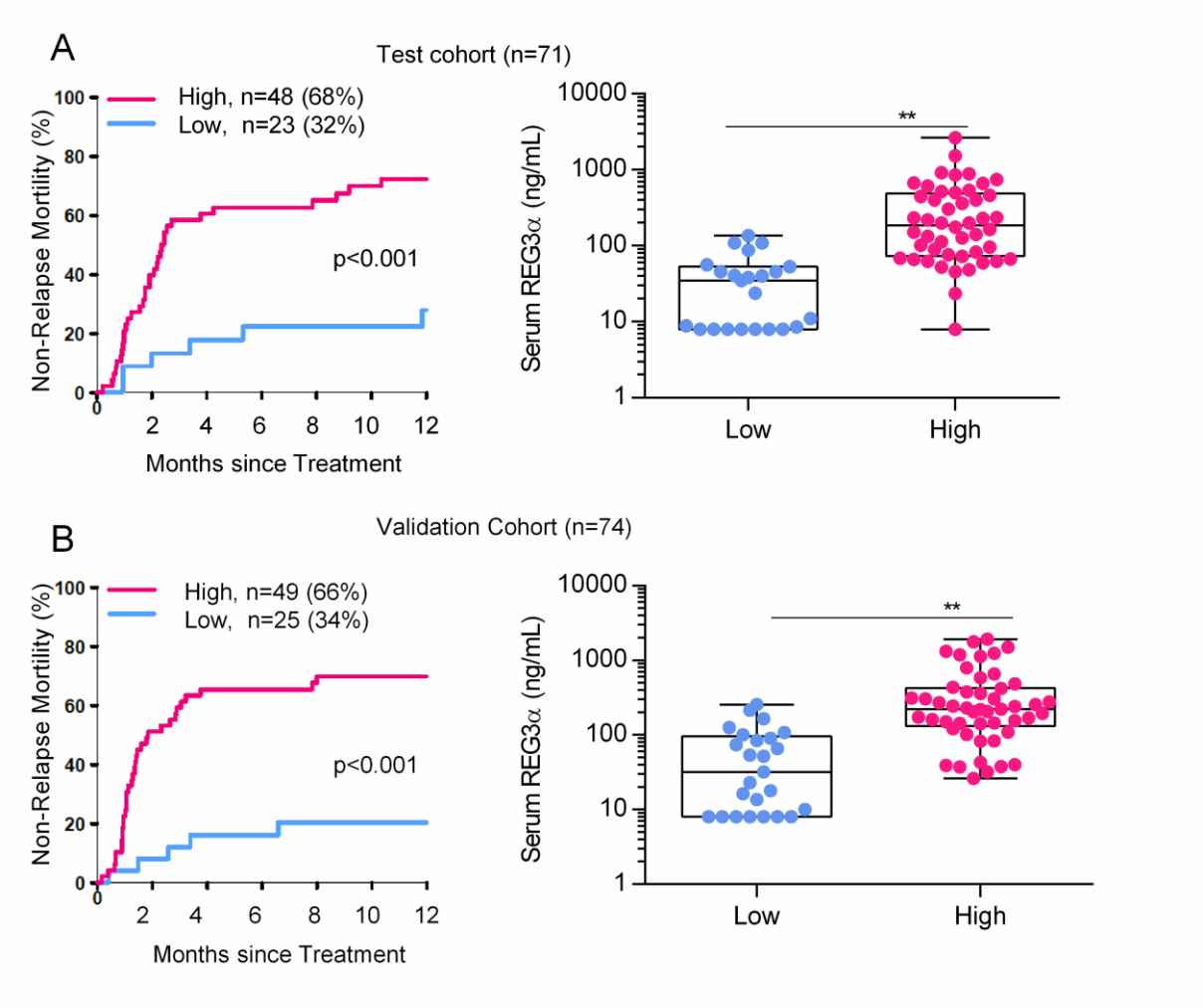

Figure 3. Serum REG3α levels and correlates with non-relapse mortality (NRM) in patients with GI GVHD. Patients with GI GVHD (n=145) who were treated with systemic steroids for at least seven days provided blood samples for biomarker analysis and were divided according to biomarker probabilities into low (■) and high (■) groups as previous published (16). 12 month NRM and REG3α serum levels were shown for (**A**) test (n=71) and (**B**) validation (n=74) cohorts. **P<0.01, unpaired two-tailed *t* test. Data are expressed as Box and Whisker plots.

Figure 4

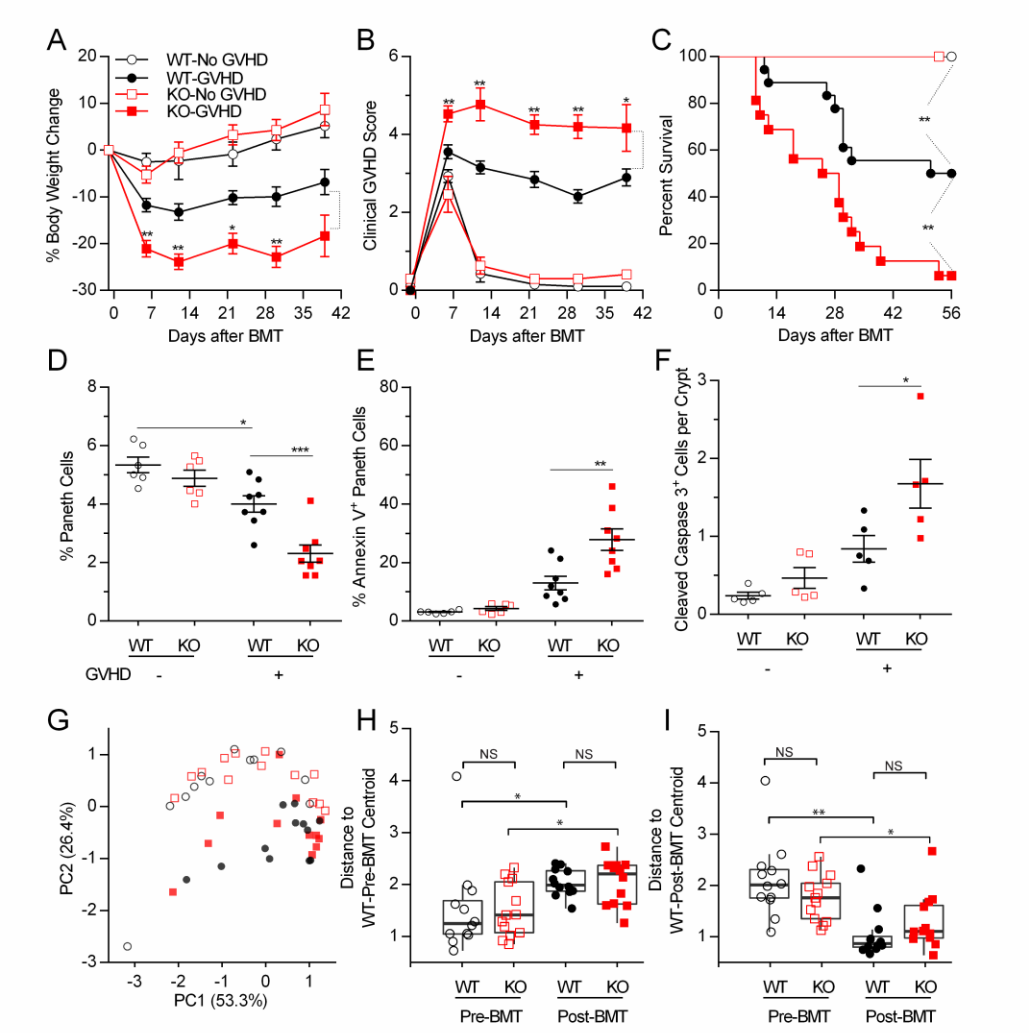

Figure 4. REG3γ absence increases GVHD severity. Wild type B6 (WT) and B6-*Reg3g*$^{-/-}$ (KO) mice underwent BMT from B6-Ly5.1 donors (GVHD −: WT ○, KO □) or C3H.SW donors (GVHD +: WT ●, KO ■). **(A)** Serial body weight measurement, **(B)** clinical GVHD score and **(C)** survival of mice after BMT (WT ○, n=7; KO □, n=7; WT ●, n=18; KO ■, n=16). **P<0.01, log-rank test. **(D-F)** On day +7 after BMT, WT or KO recipients (Lgr5-EGFP^{+}) were euthanized. Small intestine crypt cells were isolated and analyzed by flow cytometry. Small intestine sections were stained by immunochemistry. **(D)** Quantification of Paneth cells and **(E)** Quantification of Paneth cells undergoing early apoptosis by Annexin V^{+} staining (WT ○, n=6; KO □, n=6; WT ●, n=8; KO ■, n=8). **(F)** Quantification of cleaved Caspase-3^{+} cells per crypt of ileum sections in recipients (each group, n=5).*P<0.05, **P<0.01, ***P<0.001, unpaired two-tailed *t* test (**A,B,D,E,F**). Data are expressed as mean ±SEM. **(G-I)** Microbiome composition of fecal samples from WT and KO mice on one day before BMT (Pre-BMT) (WT ○, n=12; KO □, n=13) or day +7 after BMT (Post-BMT) (WT ●, n=12; KO ■, n=13). **(G)** Principal Component Analysis (PCA) was computed from the Bray-Curtis beta-diversity matrix among all samples. **(H)** Bray-Curtis compositional distances were measured from the centroid of WT Pre-BMT samples or **(I)** Post-BMT samples. NS= P>0.05, *P<0.05, **P<0.01, Wilcox test.

Figure 5

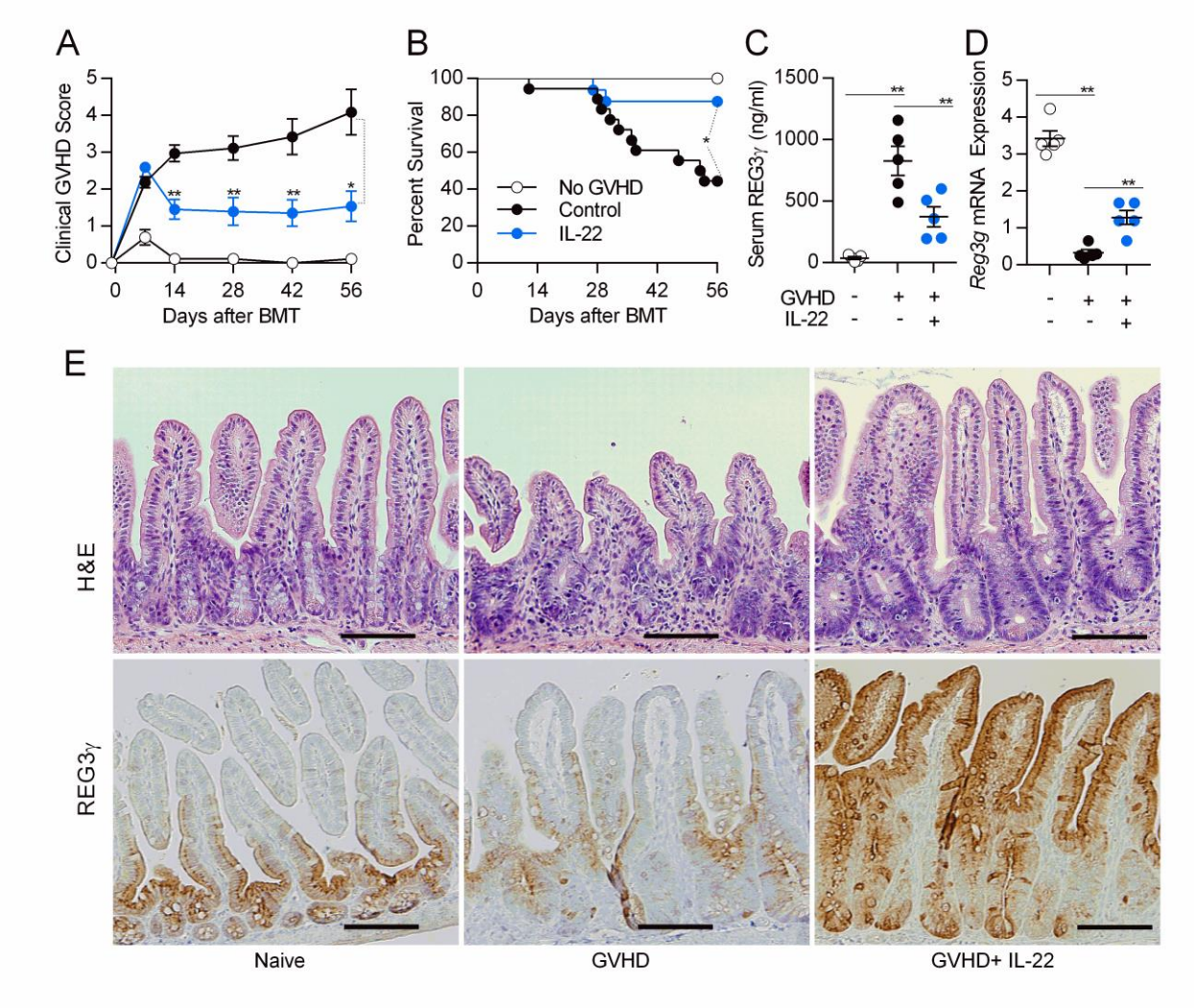

Figure 5. Prophylactic administration of IL-22 reduces GVHD. B6D2F1 mice received PBS or IL-22 injections from day +1 after BMT from B6 donors (GVHD, +) or B6D2F1 donors (No GVHD, −). **(A)** Clinical GVHD score and **(B)** Survival of mice after BMT (GVHD +: PBS ●, n=18; IL-22 ●, n=16; GVHD − ○, n=7). *P<0.05, log-rank test. **(C-E)** Samples were analyzed on day +7 after BMT. **(C)** Serum REG3γ levels, **(D)** Ileal tissue *Reg3g* mRNA expression. .*P<0.05, **P<0.01, unpaired two-tailed *t* test (**A**) one-way ANOVA (**C,D**). **(E)** Hematoxylin and Eosin (H&E, top) staining and REG3γ (bottom) staining by immunohistochemistry in ileum from individual mice with or without IL-22 treatment. Naïve B6D2F1 mice were used as controls. Images were taken with an Olympus BX51 with a 20x objective. Scale bars are 100 µm. Data are expressed as mean ±SEM.

Figure 6

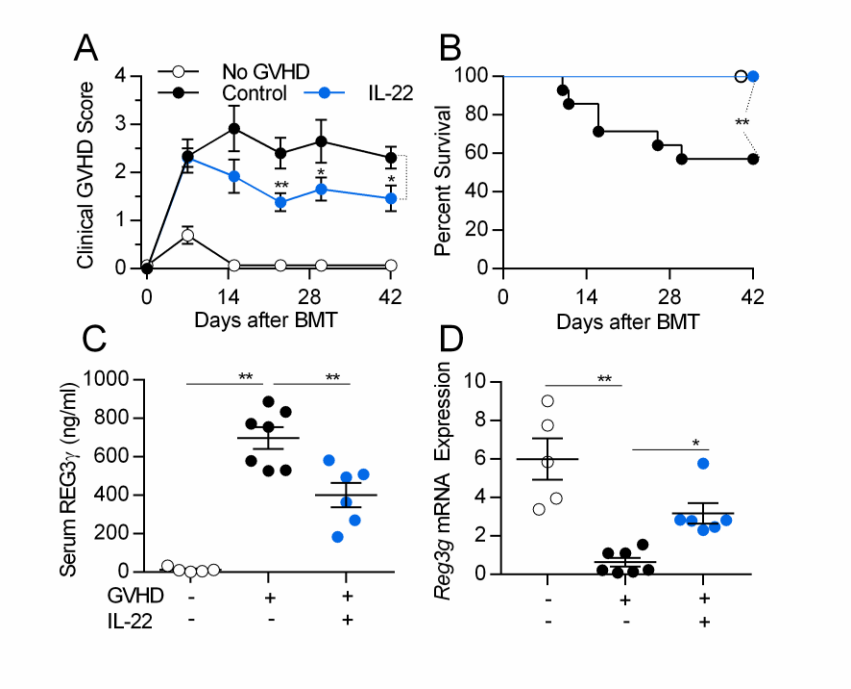

Figure 6. IL-22 treatment reverses GVHD. B6 mice received BM and T cells from C3H.SW donors (GVHD +), treated with PBS (PBS ●) or IL-22 (IL-22 ●) from day +7. As a control, mice received BM only (No GVHD − ○). **(A)** Clinical GVHD score and **(B)** Survival of mice after BMT (PBS ●, n=14; IL-22 ●, n=13; No GVHD ○, n=5).). Samples were analyzed on day +10. **P<0.01, log-rank test. (**C**) Serum REG3γ protein and (**D**) small intestine tissue *Reg3g* mRNA. *P<0.05, **P<0.01, unpaired two-tailed *t* test (**A**) one-way ANOVA (**C,D**). Data are expressed as mean ±SEM.

Figure 7

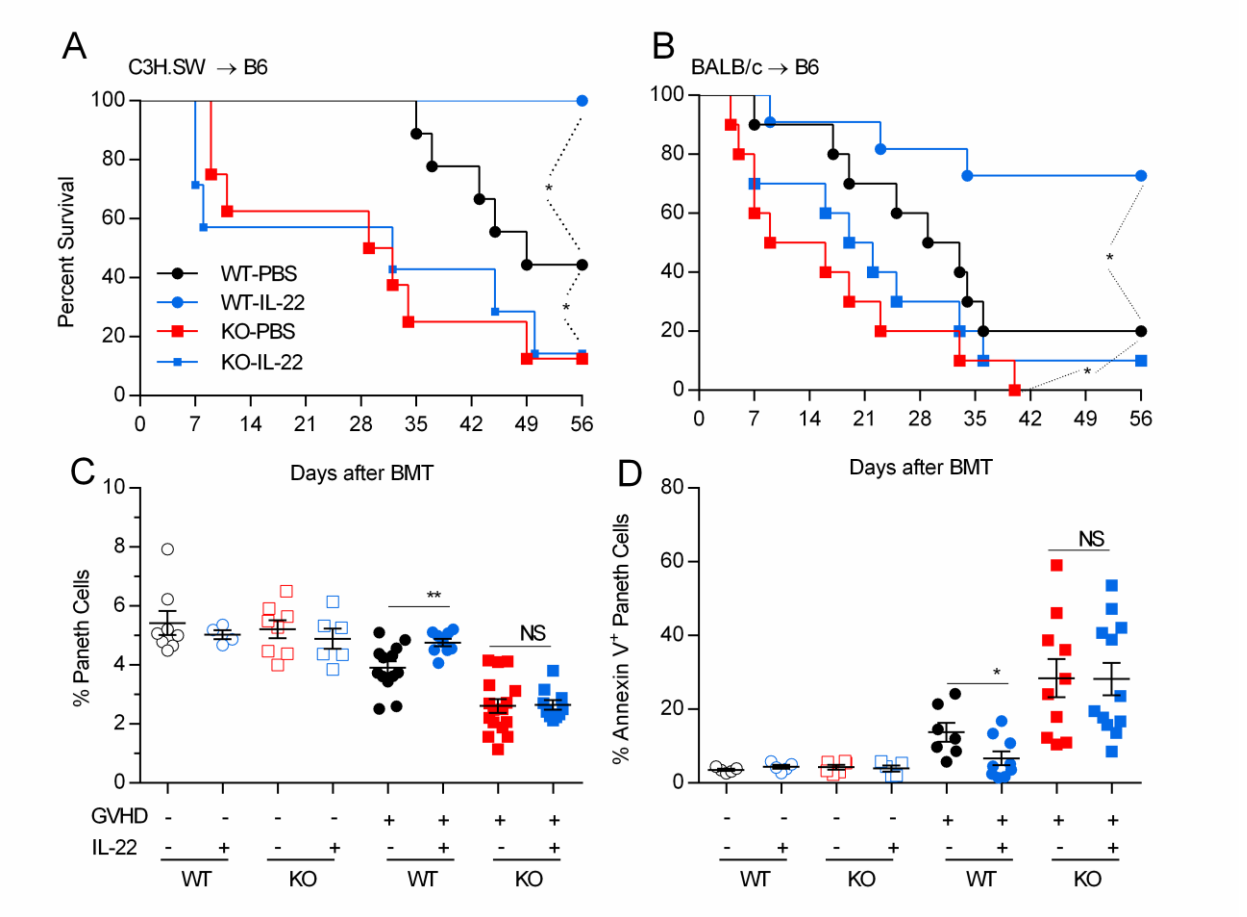

Figure 7. IL-22 requires REG3γ to reduce GVHD. (A) Survival of wild type B6 (WT) and B6-*Reg3g*$^{-/-}$ (KO) mice received PBS or IL-22 injections from day +1 after BMT from C3H.SW donors (WT PBS ●, n=9; WT IL-22 ●, n=8; KO PBS ■, n=8; KO IL-22 ■, n=7). **(B)** Survival of wild type B6 (WT) and B6- *Reg3g*$^{-/-}$ (KO) mice received PBS or IL-22 injections from day +1 after BMT from BALB/c donors (WT PBS ●, n=10; WT IL-22 ●, n=11; KO PBS ■, n=10; KO IL-22 ■, n=10). *P<0.05, log-rank test. **(C,D)** Wild type B6 (WT) and B6- *Reg3g*$^{-/-}$ (KO) mice (Lgr5-EGFP^{+}) received PBS or IL-22 injections from day +1 after BMT from B6-Ly5.1 donors (GVHD −) or C3H.SW donors (GVHD +). On day +7 after BMT, small intestine crypt cells were analyzed by flow cytometry. **(C)** Quantification of Paneth cells (GVHD −: WT PBS ○, n=8; WT IL-22 ○, n=4; KO PBS □, n=8; KO IL-22 □, n=6; GVHD +: WT PBS ●, n=13; WT IL-22 ●, n=9; KO PBS ■, n=16; KO IL-22 ■, n=10). **(D)** Quantification of Paneth cells undergoing early apoptosis by Annexin V^{+} staining (GVHD −: WT PBS ○, n=5; WT IL-22 ○, n=5; KO PBS □, n=6; KO IL-22 □, n=5; GVHD +: WT PBS ●, n=7; WT IL-22 ●, n=9; KO PBS ■, n=10; KO IL-22 ■, n=12). NS=P>0.05; *P<0.05, **P<0.01, unpaired two-tailed *t* test. Data are expressed as mean ±SEM.

Figure 8

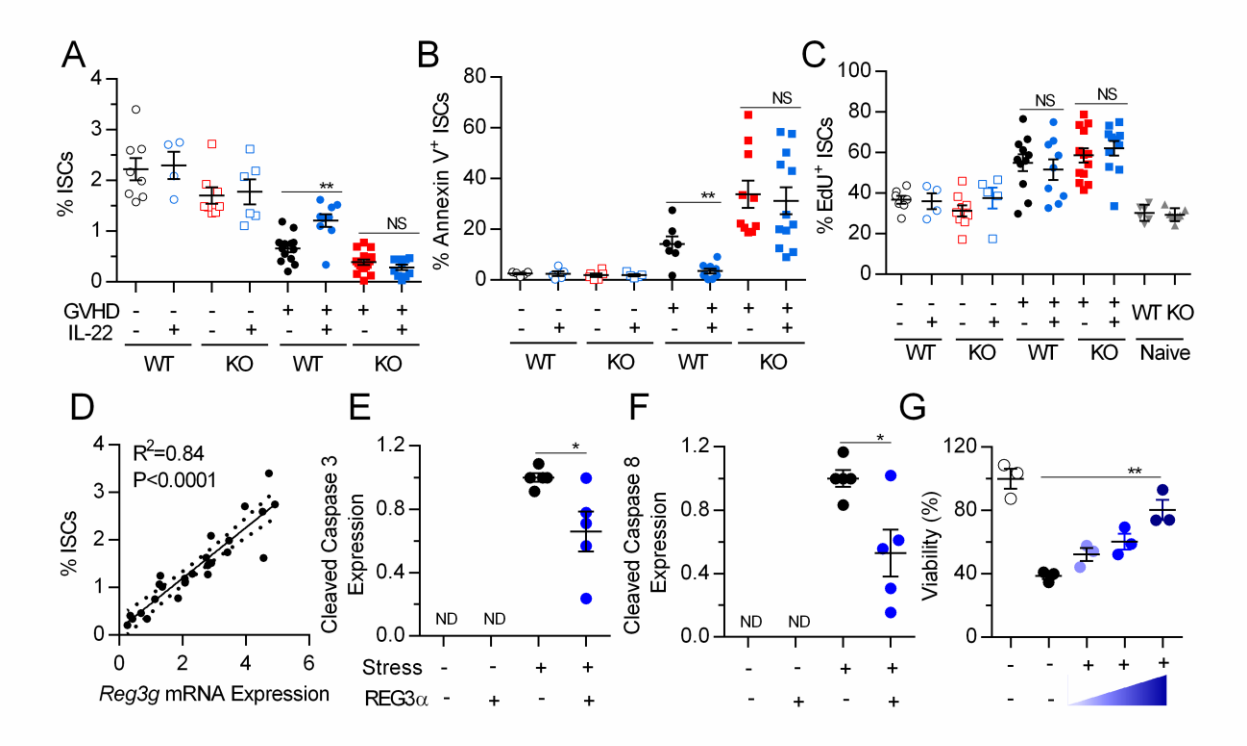

Figure 8. REG3γ protects ISCs from apoptosis. (A-D) Wild type B6 (WT) and B6- *Reg3g*$^{-/-}$ (KO) mice (Lgr5-EGFP^{+}) received PBS or IL-22 injections from day +1 after BMT from B6-Ly5.1 donors (GVHD −) or C3H.SW donors (GVHD +). On day +7 after BMT, small intestinal crypt cells were analyzed by flow cytometry and *Reg3g* mRNA was measured by qPCR. **(A)** Quantification of ISC from mice in Figure 7. **(B)** Quantification of ISCs undergoing early apoptosis by Annexin V^{+} in the mice from Figure 7. Data are combined from three separate experiments. **(C)** Quantification of EdU^{+} ISCs in syngeneic recipients (GVHD −: WT PBS ○, n=7; WT IL-22 ○, n=4; KO PBS □, n=9; KO IL-22 □, n=5), allogeneic recipients (GVHD +: WT PBS ●, n=8; WT IL-22 ●, n=9; KO PBS ■, n=13; KO IL-22 ■, n=11), and naïve WT (▼, n=5) and KO (▲, n=5) controls. **(D)** Correlation of ISC and *Reg3g* mRNAexpression in WT mice from two of the three experiments shown in panel A (n=25), as calculated by the Pearson correlation coefficient. **(E-G)** HT-29 cells were cultured with recombinant REG3α protein and apoptotic stimuli as described in Methods. Data are representative of three independent experiments. **(E,F)** Cells lysates were collected after 16 hours cell culture for western blot analysis. Quantification of **(E)** cleaved Caspase-3 and **(F)** cleaved Caspase-8 expression. **(G)** Quantification of cell viability by CellTiter-Glo 2.0 assay after 24 hours cell culture. *P<0.05, **P<0.01, unpaired two-tailed *t* test. Data are expressed as mean ±SEM, ND=not detectable.